Chemical Physics Letters 803 (2022) 139847

Contents lists available at ScienceDirect

Chemical Physics Letters

journal homepage: www.elsevier.com/locate/cplett

Research paper

Mesoscopic model confirms strong base pair metal mediated bonding for T–Hg^{2+}–T and weaker for C–Ag^{+}–C

Luciano Gabriel Silva, Gerald Weber [*]

Departamento de Física, Universidade Federal de Minas Gerais, 31270-901, Belo Horizonte - MG, Brazil

GRAPHICAL ABSTRACT

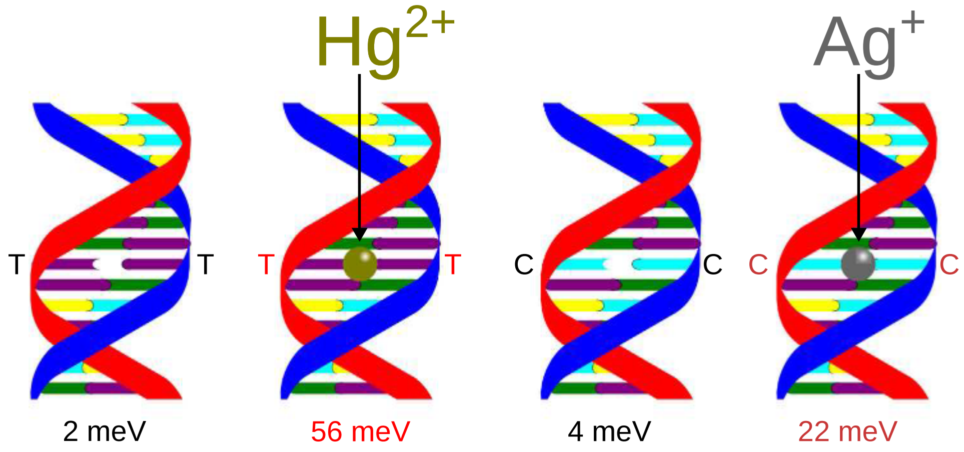

HIGHLIGHTS

- Metal mediated bond potentials were obtained for T–Hg^{2+}–T and C–Ag^{+}C.
- T–Hg^{2+}–T bond potential is of similar strength as a hydrogen bond of a CG base pair.
- C–Ag^{+}C is much weaker supporting the hypothesis of a bond of type N3–Ag^{+}–N3.
- Stacking interactions are increased only for GC–TT and CC–AT.

ARTICLE INFO

Keywords:
Metal-mediated DNA
Metallo-base-pair
Peyrard–Bishop DNA model
DNA stability
Hydrogen bonds
Stacking interaction

ABSTRACT

Metal mediated DNA are mismatches where a metal ion bridges the base pairs and are of interest for biosensors. Here, we study T–Hg^{2+}–T, which is known to be stabilized by base pair metal mediated bonds, and C–Ag^{+}–C whose stabilization mechanism is less well understood. We use a mesoscopic model and published melting temperatures of sequences containing CC or TT mismatches in the presence of the metal ions. For T–Hg^{2+}–T we obtain a strong base pair bond potential and moderate one for C–Ag^{+}–C, only one stacking potential for each configuration is stronger than usual.

---

[*] Corresponding author.
E-mail address: gweber@ufmg.br (G. Weber).

https://doi.org/10.1016/j.cplett.2022.139847
Received 1 March 2022; Received in revised form 20 June 2022; Accepted 1 July 2022

1. Introduction

Metal-mediated DNA, sometimes called M-DNA, where a metal ion occupies the hydrogen bond, typically in mismatched base pairs, has a long history, reaching back to the early 1950–60s [1–3]. Today, its continued interest lies in its potential to be used as a highly sensitive and specific metal sensor [4–7] as well as in the formation of nanowires [8–10]. The pioneering work by Ono and Miyake [11] revealed two M-DNA structures, CC mismatches mediated by Ag^+, and TT mismatches mediated by Hg^{2+}, which are still the main M-DNA structures studied. For T–Hg^{2+}–T, it was found that it yields a higher melting temperature than a canonical AT base pair [11], and its structure obtained from NMR measurements is now considered well understood [12–14]. In particular it was shown that two imino protons are released when T–Hg^{2+}–T is formed [12] and that C1′–C1′ distances are shorter than those of Watson–Crick base pairs [13,15]. Miyake et al. [16] determined that in a T–Hg^{2+}–T structure, Hg^{2+} binds directly to N3 of thymidine in place of the imino proton and bridges the thymidine residues. However, for C–Ag^+–C a number of questions regarding its structure still remain. For instance, there appear to be conflicting results suggesting either a N3–Ag^+–N3 [17], N3–Ag^+–O2 [18], or a N3–Ag^+–N3 linkage [19]. On the other hand, DFT calculations by Espinosa Leal et al. [20] suggests the existence of interplanar bonds which were also observed in crystal structures of N^1-hexylcytosine [19]. There are evidences of C–Ag^+–C base pair formation in backbone-less $[Ag(cytidine)_2]^+$ complexes [21] which were shown to form a cisoid configuration in density-functional theory (DFT) calculations by Kliuev et al. [22], however it is unclear how these finding would translate to fully formed duplexes. Other DFT calculations explore the effect of Zn^{2+} [23], which are not covered here.

Mesoscopic models, such as the Peyrard–Bishop (PB) model, uses a set of effective potentials to describe the main interactions of the DNA double helix, namely the hydrogen bonds and the stacking interactions [24]. This type of model can be used to calculate melting temperatures with similar accuracy as nearest-neighbour models [25]. These models depend critically on adjusted parameters, and we showed that these parameters can be obtained from experimental melting temperatures [26]. An additional bonus of obtaining the parameters in this way is that they can be directly related to hydrogen bonds, or base pair metal mediated bonds, and the stacking interactions. In other words, combining the mesoscopic model with experimental melting temperatures provides a way to evaluate these interactions. The method has now been validated for several oligonucleotide systems, including a recent study for all possible combinations of mismatches for which we obtained overall good correspondence to the results from other experimental methods such as NMR [27]. The new mismatch parametrization now opens an opportunity to apply the method to other systems containing mismatches in more challenging configurations, notably T–Hg^{2+}–T and C–Ag^+–C. It is of particular interest to understand if existing melting temperatures of T–Hg^{2+}–T and C–Ag^+–C would result in increased base pair Morse potentials which is the central hypothesis of metal-ion stabilization in these mismatches [16]. It would be of especial interest to determine if existing melting temperatures could advance our understanding concerning the conflicting results related to base-pair metal mediated bonding of C–Ag^+–C.

The major challenge in studying the metal mediated T–Hg^{2+}–T and C–Ag^+–C with mesoscopic models is the relative small number of melting temperatures that are scattered over a number of different studies. It is unclear if the mesoscopic model would be effective in providing a clear description of the base pair bond interactions for such a limited set of data. Furthermore, DNA mismatches are very sensitive to changes in buffer conditions and it is not clear if the existing parameters can be used as reliable starting point for the optimization of metal mediated potentials. On the other hand a successful optimization of T–Hg^{2+}–T and C–Ag^+–C would broaden the potential applications of DNA mismatch existing parameters and provide a critical validation of the method for a small melting temperature data set.

2. Materials and methods

2.1. Notation

We used the notation CC and TT for non-canonical DNA base pairs. The stacking interactions are represented by a (base pair 1)-(base pair 2) scheme. For example, the mismatch CC and the canonical pair AT, corresponding to the dimer 5′-CA-3′/3′-CT-5′, is represented by CC-AT. Note that due to symmetry considerations, as 5′-CA-3′/3′-CT-5′ is the same as 5′-TC-3′/3′-AC-5′, therefore CC–AT is same as TA–CC.

The main goal is to observe the changes in base pair bond and stacking interactions, next to the mismatch due to the presence of a metal ion. To differentiate between the presence or absence of Ag^+, or Hg^{2+}, in solution we used the following notation: sequences without metal were called control, represented by CC-CTRL and TT-CTRL; for sequences with metal we used the notation C–Ag^+–C and T–Hg^{2+}–T that is commonly used in the field.

2.2. Melting temperature data set

For C–Ag^+–C we used 22 sequences containing a concentration of 1 equivalent of Ag^+ per mismatch CC from Refs. [11,28–38] and their corresponding control sequences (CC-CTRL) without Ag^+ (21 melting temperatures). For T–Hg^{2+}–T we used 34 sequences containing 1 equivalent of Hg^{2+} per mismatch TT from Refs. [13,16,28,29,31,32,38–44] and 24 control sequences (TT-CTRL) without Hg^{2+}.

The majority of melting temperatures in these sets are at a salt concentration, $[Na^+]$, of 100 mM and total strand concentration of 2 μM. For different conditions we applied a salt correction factor, equation (22) from Owczarzy et al. [45], and recalculated the strand concentrations to 2 μM [46] from the reported experimental total enthalpy and entropy variations. Supplementary tables S1 and S2 show the melting temperatures, T_{exp}, that were adjusted in this way. The remaining buffer conditions were in general very similar among the various datasets.

2.3. Mesoscopic models

The mesoscopic Peyrard–Bishop (PB) model describes the intramolecular interactions of DNA through simple potentials [24]. For example, stacking between the nearest-neighbours base pairs is described by a harmonic potential, while the base pair bond, usually a hydrogen bond, is represented by a Morse potential. For the ith base pair the Morse potential is

$$V(y_i) = D_\alpha \left(e^{-y_i/\lambda_\alpha} - 1\right)^2, \tag{1}$$

where the parameter D_α tells us how strongly the α base pair are bonded, whereas λ_α is related to the potential width. For the nearest-neighbour stacking interaction we use a modified harmonic potential which includes a small twist angle θ [26]

$$W(y_i, y_{i-1}) = \frac{k_\beta}{2}\left(y_i^2 - 2y_i y_{i-1}\cos\theta + y_{i-1}^2\right), \tag{2}$$

where the parameter k_β is the coupling constant of nearest-neighbours of type β, and the angle is fixed at $\theta = 0.01$ rad, which is introduced to overcome well known numerical problems with the transfer-integral technique [26].

With the two potentials of Eqs. (1) and (2) we can calculate the classical partition function from which we obtain an adimensional index $\tau_i(P)$, which is proportional to the melting temperatures [26]. Additionally, we can calculate the average strand displacement $\langle y_i \rangle$ for each base pair i by calculating the expected value of y from the partition function [26].

2.4. Calculation of melting temperatures

The index $\tau_i(P)$ is used to predict melting temperatures for any sequence i, where P is a given set of parameters. Experimental melting temperatures and $\tau_i(P)$ are linearly dependent within groups of sequences of same length N. This relation is show in the following equation

$$T_i'(P) = a_0(N) + a_1(N)\tau_i(P), \tag{3}$$

where $a_{0,1}(N)$ are the linear regression coefficients. These coefficients have a linear dependence with $N^{1/2}$

$$a_k(N) = b_{0,k} + b_{1,k}N^{1/2}, \quad k = 0, 1. \tag{4}$$

2.5. Thermal equivalence optimization

The parameter optimization is carried out by minimizing the merit function

$$\chi_j^2(P_j) = \sum_{i=1}^{N} \left[T_i - T_i'(P_j)\right]^2, \tag{5}$$

where P_j is the jth tentative set of parameters. The goal is to find the best set of P_j parameters such that the calculated temperatures, $T_i'(P_j)$, are closest to the experimental temperatures, T_i. Considering that the set P contains M parameters, the numerical problem consist of finding the M-dimensional minima of Eq. (5), which is numerically implemented with a downhill simplex algorithm [25].

Another equation considered in our discussion to evaluate the quality of the prediction is the average melting temperature deviation

$$\langle \Delta T\rangle = \frac{1}{N}\sum_{i=1}^{N} |T_i - T_i'(P_j)|. \tag{6}$$

2.6. Minimization procedure

One of the main challenges in the numerical minimization of Eq. (5) is the unavoidable occurrence of local minima, that is, local valleys that do not coincide with the best overall minima. To overcome this problem, we repeat the minimization process multiple times, restarting from different initial parameters. For each minimization round, the initial set of parameters $P_{\mathrm{init.}}$ are randomly sampled around the 10% of value of seed parameters P_{seed}, that is, within the interval of $0.9P_{\mathrm{seed}}$ to $1.1P_{\mathrm{seed}}$. Only Morse potentials D and stacking potentials k were varied. The λ parameters were kept constant since we have found, in previous studies, that their effect on melting temperatures is negligible [26]. In total, 6 parameters were varied for each type of metal mediated mismatch: one Morse potential factor D and 5 stacking factors k. The CTRL-TT, CTRL-CC, C–Ag^{+}–C and T–Hg^{2+}–T were treated separately.

CTRL optimization. For CTRL sequences, the initial seed parameters were those from Ref. [27] (supplementary table S3). One problem that occurred in this particular study was that some parameters that would repeatedly tend to zero. Due to the particularities of the minimization algorithm, once a parameter reaches zero during the minimization it will remain so during the whole minimization process. This risks artificially skewing the remaining parameters to suboptimal values. On the other hand, one cannot discard the occurrence of null parameter as DNA mismatches tend to have very small Morse potentials in most cases as well as very small stacking potentials for some specific situations. To ensure that null value parameters are not algorithmic artefacts, we identified the parameters that went to zero and artificially raised their values and repeated the whole process with a mix of non-zero optimized and artificially raised values. If after successive major rounds these same parameters would again tend to zero, it would then be an indication that indeed this would be their optimal value and not an artefact of the minimization algorithm. CTRL-TT and CTRL-CC were optimized separately. The CTRL minimizations were performed 1000 times for each round, with different initial parameters. This procedure was repeated two more times, always raising null parameters to their initial values as needed. A fourth, and last, round of minimization was for estimating the influence of experimental uncertainty on our new parameters. This was done by changing the experimental temperatures by small random amounts such that the resulting standard deviation corresponds to the experimental uncertainty. We used 0.6 °C uncertainty for CTRL, which were obtained from the average reported uncertainty for each of the published measurements. Final quality parameters were $\chi^2 = 58.56$ °C^2 and $\langle \Delta T\rangle = 1.24$ °C for CTRL-CC; $\chi^2 = 144.18$ °C^2 and $\langle \Delta T\rangle = 1.79$ °C for CTRL-TT.

C–Ag^{+}–C and T–Hg^{2+}–T optimization. For the a preliminary round, we joined the datasets, CTRL-TT with T–Hg^{2+}–T, and CTRL-CC with C–Ag^{+}–C, and varied the metal mediated parameters while keeping the control parameters fixed. We call this the preliminary optimization. This has the practical effect that all melting temperatures are forced to follow the same regression parameters Eqs. (3),(4), and causes the T–Hg^{2+}–T and C–Ag^{+}–C parameters to assume values that bear some reference to the control parameters. This approach is used only to obtain seed parameters for T–Hg^{2+}–T and C–Ag^{+}–C which are shown in supplementary table S4. After this, we perform three rounds of optimization using the T–Hg^{2+}–T and C–Ag^{+}–C separately from the CTRL sets. For the last round, we proceed as for the last CTRL, assuming a 0.6 °C to evaluate the experimental uncertainty on our new parameters. Each round was performed in 1000 local minimization steps, results shown here are from the final minimization round. Final quality parameters were $\chi^2 = 111.07$ °C^2 and $\langle \Delta T\rangle = 1.86$ °C for C–Ag^{+}–C; $\chi^2 = 94.21$ °C^2 and $\langle \Delta T\rangle = 1.35$ °C for T–Hg^{2+}–T.

2.7. Availability

The metal mediated parameters calculated were included in the latest version of our free `TfReg` software [25] which can be used to verify our results. The software and the parameters are available at http://tinyurl.com/tfregufmg, for other download options see the supplementary information.

3. Results and discussion

The optimization rounds were carried out independently for T–Hg^{2+}–T and C–Ag^{+}–C, and their respective controls. In total, four rounds with 1000 different initial conditions were carried out as described in the methods section. Quality parameters for final $\langle \Delta T\rangle$ was 1.86 °C for C–Ag^{+}–C and 1.35 for T–Hg^{2+}–T which are of the same magnitude as found in previous calculations using this method in different situations, see for instance [47,48].

In Fig. 1 we show the optimized Morse potentials. For TT-CTRL the Morse potential is somewhat lower than the its seed value, in the lower range of TT mismatches that were obtained previously [27]. The CC-CTRL Morse potential is also situated at the smaller values of CC, albeit marginally larger than the TT potential. However, both potentials are very small when compared to canonical base pairs AT and CG, therefore it is not possible to say that CC is more stable than TT from these results. With the addition of Hg^{2+}, the Morse potential increases strongly, indicating a substantial base-pair metal mediated bonding, see Fig. 1. This is much higher than any known TT configuration [27] (shaded area) and roughly 4/5 of that of a CG Morse potential (70 meV) [26], which leaves very little doubt that T–Hg^{2+}–T is stabilized by a Hg^{2+} mediated bond. To understand this results, let us briefly discuss the T–Hg^{2+}–T structure. Three configurations were suggested for T–Hg^{2+}–T: N3–Hg^{2+}–N3, O2–Hg^{2+}–N3 and N3–Hg^{2+}–O4 [49]. The N3–Hg^{2+}–N3 has the oxygen atoms in opposition to each other, yet apart far enough such that the repulsive force between them may not be so strong, which could explain the large value of the Morse potential,

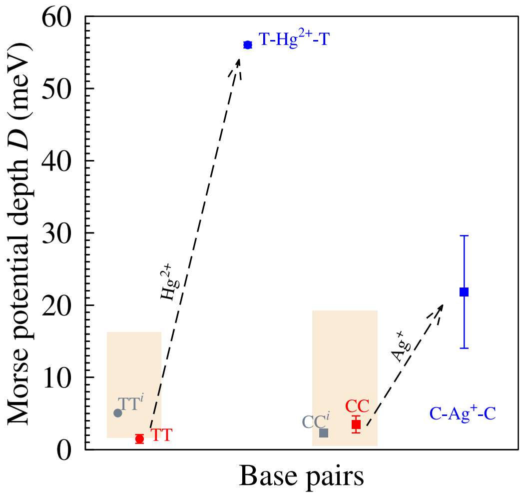

Fig. 1. Average Morse potential depths D calculated for T–Hg^{2+}–T (blue bullet) C–Ag^{+}–C (blue box) and their respective controls (red bullet and box). Error bars are the calculated standard deviation of the last minimization round. The seed values for mismatches, TT^{i} and CC^{i} (horizontally displaced for clarity), are shown as grey bullet and box, respectively. Dashed arrows indicate the changes due to the addition of cations and are only intended as guide for the eye. The shaded area shows the interval of minimum and maximum Morse potentials for all types of TT and CC mismatches from Ref. [27].

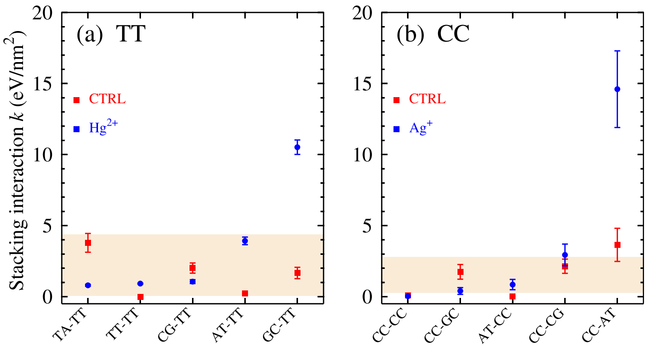

Fig. 2. Average stacking interaction k calculated for (a) T–Hg^{2+}–T and (b) C–Ag^{+}–C as blue bullets. Red boxes show the control (a) TT-CTRL and (b) CC-CTRL. Error bars are the calculated standard deviation of the last minimization round. The shaded area shows the interval of the minimum and maximum stacking interaction for equivalent mismatches from Ref. [27].

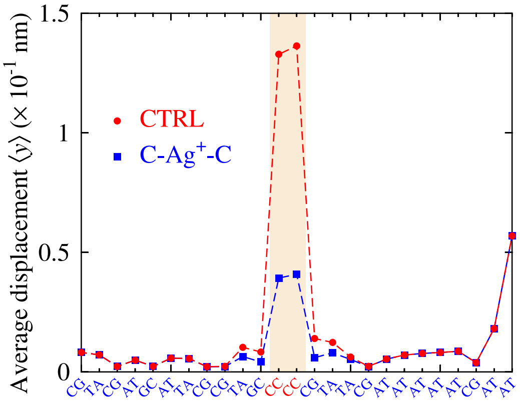

Fig. 3. Average displacement profile containing a double CC mismatch (shaded area), for the sequence from Ref. [50]. Red bullets are for CTRL parameters, and blue boxes for C–Ag^{+}–C.

Fig. 1. However, the O2–Hg^{2+}–N3 and the N3–Hg^{2+}–O4 structures are possible as well. While our model is not able to identify the structure, it clearly points to the one that is likely to be the most strongly bonded. The addition of Ag^{+} increases the CC Morse potential as well, Fig. 1. While this increase is much less than for T–Hg^{2+}–T, it is nevertheless substantial, roughly 2/3 of that of an AT Morse potential (34 meV), which suggest a single link similar to the N3–Ag^{+}–N3 link proposed by [17,19]. Such weaker Morse potential is likely due to the proximity of the repulsive amino groups facing each other at C–Ag^{+}–C, resulting in large propeller twist angles [17]. Other types of links that were suggested, such as N3–Ag^{+}–O2 linkage [18] would have an extra hydrogen bond which seems unlikely given the moderate Morse potential that was found.

From the Morse potential results, there is little doubt that T–Hg^{2+}–T is stabilized by a metal-mediated planar base pair bond, while C–Ag^{+}–C is less so. But what then explains the large increase in melting temperature when Ag^{+} is added? The first sequences shown in supplementary table S1 provide a clue to what might be happening, these are 6 sequences of same length with a central CC and where only the nearest-neighbours change. For ACA/TCT central trimer, there is an increase of 10 °C while for CCG/GCC it is only 2 °C. This large difference indicates that nearest-neighbour interactions have an important role to play in the stability. The nearest-neighbour interaction is modelled here by elastic constants k, Eq. (2), which in general are associated to stacking interaction. Our results for the stacking constants k are shown in Fig. 2 for both T–Hg^{2+}–T and C–Ag^{+}–C. By far, the highest stacking interaction is for CC-AT nearest neighbours, exactly the type present in ACA/TCT. Interestingly, the other nearest neighbours AT-CC of the ACA/TCT trimer has a very weak interaction. CC-CC, that is, for two consecutive CC mismatches the stacking interaction is almost non-existent, which means that here the increased stability is entirely driven by in-planar base pair bonds. Inter-planar Hydrogen bonds have been predicted from DFT calculations for backbone-free C–Ag^{+}–C tetramers [20] and observed in crystal structures for N^{1}-hexylcytosine [19], therefore one would have expected some degree of nearest-neighbour interaction in this case. Fig. 3 shows an average displacement profile containing a double CC mismatch. This type of profile, which is calculated as described in Ref. [25], considers the combined effects of Morse potentials and stacking, providing qualitative information regarding the regions where the base pairs are more likely to denature first. Typically, larger displacements means that the base pairs in question are less stable and will open before others. In the case of Fig. 3, the displacement profiles for C–Ag^{+}–C (blue boxes) are much smaller, indicating increased base-pair stability as compared to the CTRL-CC (red bullets).

For T–Hg^{2+}–T, the stacking interaction parameters shown in Fig. 2, only one strongly increased stacking for GC-TT was found, much higher than those previously seen for TT mismatches (shaded area) [27]. AT-TT is moderately increased in comparison to CTRL, while TA-TT is very small, even though its CTRL counterpart is relatively large. In Fig. 4a we show the average opening profiles for a sequence containing a double TT mismatch, flanked by AT-TT on both sides (note that AT-TT is equivalent to TT-TA). The CTRL displays very large displacements in the mismatch region (shaded area) while the addition of Hg^{2+} causes a complete stabilization (very small displacements). By replacing AT-TT with TA-TT, as shown in Fig. 4b, we observe only a slight disturbance in the opening profiles due to the much smaller stacking, but not enough to cause major destabilization. Clearly, the T–Hg^{2+}–T Morse potential is strong enough to compensate for the low TA-TT stacking.

The robustness of results presented here are encouraging and should enable us to apply the method to other configurations, such as for C–Hg^{2+}–T mediated base pairs. A limited amount of melting temperatures are already available, see for instance Funai et al. [30], but not in sufficiently diverse sequence variations and lengths. Here, the smallest set was for C–Ag^{+}–C with 22 sequences, which is in the lower

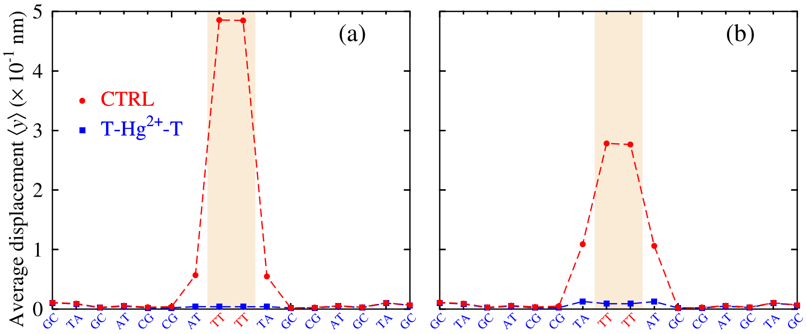

Fig. 4. Average displacement profile containing a double TT mismatch (shaded area) for the sequence from Ref. [16], panel (a). In panel (b) AT-TT was replaced with TA-TT. Red bullets are for CTRL parameters, and blue boxes for T–Hg^{2+}–T.

limit of the method. Another aspect of interest is cation concentration, here we used the available temperatures measured at one equivalent cation per mismatch, and of course zero for the controls. It would be desirable to repeat this for a larger range of concentrations which should give us a more detailed insight of the stabilization process induced by the cations. We hope that our results may stimulate further melting temperature measurements of metal mediated base pairs.

4. Conclusion

We analysed published melting temperatures for metal mediated base pairs T–Hg^{2+}–T and C–Ag^{+}–C. For T–Hg^{2+}–T we found a large Morse potential of the order of a CG base pair, while for C–Ag^{+}–C this was much smaller, roughly 2/3 of a AT base pair. For C–Ag^{+}–C, the weaker Morse potential favours the N3–Ag^{+}–N3 link proposed by [17]. For a double CC mismatch the stacking interaction was found to be very weak in the presence of Ag^{+}, but still the Morse potential was strong enough to provide some stability when compared to the absence of Ag^{+}. Very low stacking was also found for TA-TT nearest-neighbours, however due to the large T–Hg^{2+}–T Morse potential this does not affect the duplex stability.

Our results are generally in good agreement with the existing knowledge of T–Hg^{2+}–T and C–Ag^{+}–C mediated base pairs. Therefore, we believe that it should be possible to extend the method to other types of metal-mediated base pairs, for instance C–Hg^{2+}–T, when a sufficient amount of melting temperatures become available.

CRediT authorship contribution statement

Luciano Gabriel Silva: Conceptualization, Methodology, Formal analysis, Investigation, Writing – original draft, Visualization. **Gerald Weber:** Conceptualization, Methodology, Supervision, Writing – original draft, Visualization, Project administration.

Declaration of competing interest

The authors declare that they have no known competing financial interests or personal relationships that could have appeared to influence the work reported in this paper.

Data availability

Links to the data can be found in the supplementary material.

Acknowledgements

Supported by Conselho Nacional de Desenvolvimento Científico e Tecnológico (CNPq), Brazil and Coordenação de Aperfeiçoamento de Pessoal de Nível Superior (Capes, Brazil, Finance Code 001).

Appendix A. Supplementary data

Tables S1 and S2 show the sequences and temperatures used. Tables S3 and S4 show the seed parameters used.

Supplementary material related to this article can be found online at https://doi.org/10.1016/j.cplett.2022.139847.

References

[1] S. Katz, The reversible reaction of sodium thymonucleate and mercuric chloride, J. Am. Chem. Soc. 74 (9) (1952) 2238–2245, http://dx.doi.org/10.1021/ja01129a023.

[2] T. Yamane, N. Davidson, On the complexing of desoxyribonucleic acid (DNA) by mercuric ion1, J. Am. Chem. Soc. 83 (12) (1961) 2599–2607, http://dx.doi.org/10.1021/ja01473a001.

[3] M. Daune, C. Dekker, H. Schachman, Complexes of silver ion with natural and synthetic polynucleotides, Biopoly 4 (1) (1966) 51–76, http://dx.doi.org/10.1002/bip.1966.360040107.

[4] A. Ono, H. Togashi, Highly selective oligonucleotide-based sensor for mercury (II) in aqueous solutions, Angew. Chem. Int. Ed. Engl. 116 (33) (2004) 4400–4402, http://dx.doi.org/10.1002/anie.200454172.

[5] W. Zhou, R. Saran, J. Liu, Metal sensing by DNA, Chem. Rev. 117 (12) (2017) 8272–8325, http://dx.doi.org/10.1021/acs.chemrev.7b00063.

[6] V.G. Kanellis, C.G. Dos Remedios, A review of heavy metal cation binding to deoxyribonucleic acids for the creation of chemical sensors, Biophys. Rev. 10 (5) (2018) 1401–1414, http://dx.doi.org/10.1007/s12551-018-0455-y.

[7] J. Müller, Nucleic acid duplexes with metal-mediated base pairs and their structures, Coord. Chem. Rev. 393 (2019) 37–47, http://dx.doi.org/10.1016/j.ccr.2019.05.007.

[8] G.H. Clever, M. Shionoya, Metal-base pairing in DNA, Coord. Chem. Rev. 254 (19–20) (2010) 2391–2402, http://dx.doi.org/10.1016/j.ccr.2010.04.014.

[9] J. Kondo, Y. Tada, T. Dairaku, Y. Hattori, H. Saneyoshi, A. Ono, Y. Tanaka, A metallo-DNA nanowire with uninterrupted one-dimensional silver array, Nature Chem. 9 (10) (2017) 956–960, http://dx.doi.org/10.1038/NCHEM.2808.

[10] S. Vecchioni, M.C. Capece, E. Toomey, L. Nguyen, A. Ray, A. Greenberg, K. Fujishima, J. Urbina, I.G. Paulino-Lima, V. Pinheiro, J. Shih, G. Wessel, S.J. Wind, L. Rothschild, Construction and characterization of metal ion-containing DNA nanowires for synthetic biology and nanotechnology, Sci. Rep. 9 (1) http://dx.doi.org/10.1038/s41598-019-43316-1.

[11] A. Ono, Y. Miyake, Highly selective binding of metal ions to thymine-thymine and cytosine–cytosine base pairs in DNA duplexes, Nucleic Acids Res. Suppl. 3 (2003) 227–228, http://dx.doi.org/10.1093/nass/3.1.227.

[12] Y. Tanaka, S. Oda, H. Yamaguchi, Y. Kondo, C. Kojima, A. Ono, ^{15}N–^{15}N *J*-coupling across Hg^{II}: direct observation of Hg^{II}-mediated T–T base pairs in a DNA duplex, J. Am. Chem. Soc. 129 (2) (2007) 244–245, http://dx.doi.org/10.1021/ja065552h.

[13] H. Yamaguchi, J. Šbera, J. Kondo, S. Oda, T. Komuro, T. Kawamura, T. Dairaku, Y. Kondo, I. Okamoto, A. Ono, et al., The structure of metallo-DNA with consecutive thymine–Hg^{II}–thymine base pairs explains positive entropy for the metallo base pair formation, Nucleic Acids Res. 42 (6) (2014) 4094–4099, http://dx.doi.org/10.1093/nar/gkt1344.

[14] Y. Tanaka, J. Kondo, V. Sychrovskỳ, J. Šbera, T. Dairaku, H. Saneyoshi, H. Urata, H. Torigoe, A. Ono, Structures, physicochemical properties, and applications of T–Hg II–T, C–Ag I–C, and other metallo-base-pairs, Chem. Commun. 51 (98) (2015) 17343–17360, http://dx.doi.org/10.1039/C5CC02693H.

[15] J. Kondo, T. Yamada, C. Hirose, I. Okamoto, Y. Tanaka, A. Ono, Crystal structure of metallo DNA duplex containing consecutive Watson–Crick-like T–Hg^{II}–T Base Pairs, Angew. Chem. Int. Ed. Engl. 53 (9) (2014) 2385–2388, http://dx.doi.org/10.1002/anie.201309066.

[16] Y. Miyake, H. Togashi, M. Tashiro, H. Yamaguchi, S. Oda, M. Kudo, Y. Tanaka, Y. Kondo, R. Sawa, T. Fujimoto, et al., Mercury^{II}-mediated formation of thymine-Hg^{II}-thymine base pairs in DNA duplexes, J. Am. Chem. Soc. 128 (7) (2006) 2172–2173, http://dx.doi.org/10.1021/ja056354d.

[17] T. Dairaku, K. Furuita, H. Sato, J. Šebera, K. Nakashima, J. Kondo, D. Yamanaka, Y. Kondo, I. Okamoto, A. Ono, et al., Structure determination of an Ag^{I}-Mediated Cytosine–Cytosine Base Pair within DNA Duplex in Solution with $^{1}H/^{15}N/^{109}Ag$ NMR Spectroscopy, Chem. — Eur. J. 22 (37) (2016) 13028–13031, http://dx.doi.org/10.1002/chem.201603048.

[18] Y. Wang, B. Ritzo, L.-Q. Gu, Silver (I) ions modulate the stability of DNA duplexes containing cytosine, methylcytosine and hydroxymethylcytosine at different salt concentrations, RSC Adv. 5 (4) (2015) 2655–2658, http://dx.doi.org/10.1039/c4ra14490b.

[19] A. Terrón, B. Moreno-Vachiano, A. Bauzá, A. García-Raso, J.J. Fiol, M. Barceló-Oliver, E. Molins, A. Frontera, X-ray Crystal structure of a metalled double-helix generated by infinite and consecutive C^{*}-Ag^{I}-C^{*} (C^{*}:N^{1}-Hexylcytosine) base pairs through argentophilic and hydrogen bond interactions, Chem. — Eur. J. 23 (9) (2017) 2103–2108, http://dx.doi.org/10.1002/chem.201604331.

[20] L.A. Espinosa Leal, A. Karpenko, S. Swasey, E.G. Gwinn, V. Rojas-Cervellera, C. Rovira, O. Lopez-Acevedo, The role of hydrogen bonds in the stabilization of silver-mediated cytosine tetramers, J. Phys. Chem. Lett. 6 (20) (2015) 4061–4066, http://dx.doi.org/10.1021/acs.jpclett.5b01864.

[21] T. Dairaku, R. Kawai, T. Kanaba, T. Ono, K. Yoshida, H. Sato, K. Nozawa-Kumada, Y. Kondo, J. Kondo, A. Ono, et al., Effect of cytosine–Ag^{+}–cytosine base pairing on the redox potential of the Ag^{+}/Ag couple and the chemical reduction of Ag^{+} to Ag by tetrathiafulvalene, Dalton Trans. 50 (22) (2021) 7633–7639, http://dx.doi.org/10.1039/d1dt00975c.

[22] P.N. Kliuev, P.A. Sokolov, R.R. Ramazanov, QM/MM-MD dissociation of Ag+ and H+ mediated cytosine pairs: Monomers and dimers, J. Organomet. Chem. 919 (2020) 121333, http://dx.doi.org/10.1016/j.jorganchem.2020.121333.

[23] S.S. Alexandre, B.J. Murta, J.M. Soler, F. Zamora, Stability and electronic structure of M-DNA: Role of metal position, Phys. Rev. B 84 (4) (2011) 045413, http://dx.doi.org/10.1103/PhysRevB.84.045413.

[24] M. Peyrard, A.R. Bishop, Statistical mechanics of a nonlinear model for DNA denaturation, Phys. Rev. Lett. 62 (23) (1989) 2755–2757, http://dx.doi.org/10.1103/PhysRevLett.62.2755.

[25] G. Weber, Tfreg: Calculating DNA and RNA melting temperatures and opening profiles with mesoscopic models, Bioinformatics 29 (2013) 1345–1347, http://dx.doi.org/10.1093/bioinformatics/btt133, http://bioinformatics.oxfordjournals.org/content/29/10/1345.

[26] G. Weber, J.W. Essex, C. Neylon, Probing the microscopic flexibility of DNA from melting temperatures, Nat. Phys. 5 (2009) 769–773, http://dx.doi.org/10.1038/nphys1371.

[27] L.M. Oliveira, A.S. Long, T. Brown, K.R. Fox, G. Weber, Melting temperature measurement and mesoscopic evaluation of single double and triple DNA Mismatches, Chem. Sci. 11 (2020) 8273–8287, http://dx.doi.org/10.1039/d0sc01700k, https://pubs.rsc.org/en/content/articlelanding/2020/SC/D0SC01700K.

[28] A. Ono, H. Torigoe, Y. Tanaka, I. Okamoto, Binding of metal ions by pyrimidine base pairs in DNA duplexes, Chem. Soc. Rev. 40 (12) (2011) 5855–5866, http://dx.doi.org/10.1039/c1cs15149e.

[29] T. Funai, N. Adachi, M. Aotani, S. i. Wada, H. Urata, Effects of metal ions on thermal stabilities of DNA duplexes containing homo-and heterochiral mismatched base pairs: comparison of internal and terminal substitutions, Nucleos. Nucleot. Nucl. 39 (1–3) (2020a) 310–321, http://dx.doi.org/10.1080/15257770.2019.1658116.

[30] T. Funai, M. Aotani, R. Kiriu, J. Nakamura, Y. Miyazaki, O. Nakagawa, S. i. Wada, H. Torigoe, A. Ono, H. Urata, Silver (I)-ion-mediated cytosine-containing base pairs: Metal ion specificity for duplex stabilization and susceptibility toward DNA Polymerases, ChemBioChem 21 (4) (2020b) 517–522, http://dx.doi.org/10.1002/cbic.201900450.

[31] H. Urata, E. Yamaguchi, Y. Nakamura, S. i. Wada, Pyrimidine–pyrimidine base pairs stabilized by silver (I) ions, Chem. Commun. 47 (3) (2011) 941–943, http://dx.doi.org/10.1039/C0CC04091F.

[32] O. Nakagawa, A. Fujii, Y. Kishimoto, Y. Nakatsuji, N. Nozaki, S. Obika, 2′O, 4′C-methylene-bridged nucleic acids stabilize metal-mediated base pairing in a DNA duplex, ChemBioChem 19 (22) (2018) 2372–2379, http://dx.doi.org/10.1002/cbic.201800448.

[33] A. Ono, S. Cao, H. Togashi, M. Tashiro, T. Fujimoto, T. Machinami, S. Oda, Y. Miyake, I. Okamoto, Y. Tanaka, Specific interactions between silver (I) ions and cytosine–cytosine pairs in DNA duplexes, Chem. Commun. (39) (2008) 4825–4827, http://dx.doi.org/10.1039/B808686A.

[34] N. Zimmermann, E. Meggers, P.G. Schultz, A novel silver (I)-mediated DNA base pair, J. Am. Chem. Soc. 124 (46) (2002) 13684–13685, http://dx.doi.org/10.1021/ja0279951.

[35] I. Schönrath, V.B. Tsvetkov, T.S. Zatsepin, A.V. Aralov, J. Müller, Silver (I)-mediated base pairing in parallel-stranded DNA involving the luminescent cytosine analog 1, 3-diaza-2-oxophenoxazine, JBIC, J. Biol. Inorg. Chem. 24 (5) (2019) 693–702, http://dx.doi.org/10.1007/s00775-019-01682-1.

[36] H. Torigoe, Y. Miyakawa, A. Ono, T. Kozasa, Thermodynamic properties of the specific binding between Ag+ ions and C: C mismatched base pairs in duplex DNA, Nucleos. Nucleot. Nucl. 30 (2) (2011a) 149–167, http://dx.doi.org/10.1080/15257770.2011.553210.

[37] S. Naskar, M. Hebenbrock, J. Müller, Light-induced formation of silver (I)-mediated base pairs in DNA: Possibilities and limitations, Inorg. Chim. Acta 512 (2020) 119856, http://dx.doi.org/10.1016/j.ica.2020.119856.

[38] A. Fujii, O. Nakagawa, Y. Kishimoto, T. Okuda, Y. Nakatsuji, N. Nozaki, Y. Kasahara, S. Obika, A, 1, 3, 9-Triaza-2-oxophenoxazine: An artificial nucleobase forming highly stable self-base pairs with three Ag^{I} ions in a duplex, Chem. — Eur. J. 25 (31) (2019) 7443–7448, http://dx.doi.org/10.1002/chem.201900373.

[39] H. Torigoe, A. Ono, T. Kozasa, Hg^{II} ion specifically binds with T:T mismatched base pair in duplex DNA, Chem. — Eur. J. 16 (44) (2010) 13218–13225, http://dx.doi.org/10.1002/chem.201001171.

[40] O.P. Schmidt, S. Jurt, S. Johannsen, A. Karimi, R.K. Sigel, N.W. Luedtke, Concerted dynamics of metallo-base pairs in an A/B-form helical transition, Nuovo Cimento 10 (2019) 4818, http://dx.doi.org/10.1038/s41467-019-12440-x.

[41] T. Funai, C. Tagawa, O. Nakagawa, S. i. Wada, A. Ono, H. Urata, Enzymatic formation of consecutive thymine–Hg^{II}–thymine base pairs by DNA polymerases, Chem. Commun. 56 (2020c) 12025, http://dx.doi.org/10.1039/d0cc04423g.

[42] G. Mata, O.P. Schmidt, N.W. Luedtke, A fluorescent surrogate of thymidine in duplex DNA, Chem. Commun. 52 (25) (2016) 4718–4721, http://dx.doi.org/10.1039/c5cc09552b.

[43] O.P. Schmidt, A.S. Benz, G. Mata, N.W. Luedtke, Hg^{II} binds to C–T mismatches with high affinity, Nucleic Acids Res. 46 (13) (2018) 6470–6479, http://dx.doi.org/10.1093/nar/gky499.

[44] J.H. Han, S. Hirashima, S. Park, H. Sugiyama, Highly sensitive and selective mercury sensor based on mismatched base pairing with ^{diox}T, Chem. Commun. 55 (69) (2019) 10245–10248, http://dx.doi.org/10.1039/c9cc05123f.

[45] R. Owczarzy, Y. You, B.G. Moreira, J.A. Manthey, L. Huang, M.A. Behlke, J.A. Walder, Effects of sodium ions on DNA duplex oligomers: improved predictions of melting temperatures, Biochem 43 (2004) 3537–3554, http://dx.doi.org/10.1021/bi034621r.

[46] S. Schreiber-Gosche, R.A. Edwards, Thermodynamics of oligonucleotide duplex melting, J. Chem. Educ. 86 (5) (2009) 644, http://dx.doi.org/10.1021/ed086p644.

[47] E.d.O. Martins, V.B. Barbosa, G. Weber, DNA/RNA Hybrid mesoscopic model shows strong stability dependence with deoxypyrimidine content and stacking interactions similar to RNA/rna, Chem. Phys. Lett. 715C (2019) 14–19, http://dx.doi.org/10.1016/j.cplett.2018.11.015.

[48] M.I. Muniz, H.H. Lackey, J.M. Heemstra, G. Weber, DNA/TNA Mesoscopic modeling of melting temperatures suggest weaker hydrogen bonding of CG than in DNA/rna, Chem. Phys. Lett. (2020) 137413, http://dx.doi.org/10.1016/j.cplett.2020.137413, https://www.sciencedirect.com/science/article/abs/pii/S0009261420303286.

[49] H. Liu, C. Cai, P. Haruehanroengra, Q. Yao, Y. Chen, C. Yang, Q. Luo, B. Wu, J. Li, J. Ma, et al., Flexibility and stabilization of Hg^{II}-mediated C:T and T:T base pairs in DNA duplex, Nucleic Acids Res. 45 (5) (2017) 2910–2918, http://dx.doi.org/10.1093/nar/gkw1296.

[50] H. Torigoe, Y. Miyakawa, A. Ono, T. Kozasa, Thermodynamic properties of the specific binding between Ag+ ions and C:C mismatched base pairs in duplex DNA, Nucleos. Nucleot. Nucl. 30 (2) (2011b) 149–167, http://dx.doi.org/10.1080/15257770.2011.553210.